



4-3-23

**TWO-DIMENSIONAL EFFECTIVE STRESS ANALYSIS
USING CONSTITUTIVE MODEL OF SOIL
UNDER ARBITRARY STRESS CONDITION**

Kiyoshi FUKUTAKE¹ and Akira OHTSUKI¹

¹ Ohsaki Research Institute, Shimizu Corporation,
Chiyodaku, Tokyo, Japan

SUMMARY

In order to simulate ground motions under arbitrary stress condition including the principal stress rotation, the authors incorporate a proper constitutive equation into dynamic analyses using two-dimensional effective stress method. A parameter for the stress reversal is proposed to distinguish the reversal shearing from the monotonous shearing. This parameter is introduced to the Matsuoka's constitutive model (1986) that can evaluate the yielding due to the principal stress rotation. The accuracy of the present method is discussed by comparing its numerical results with those by the simple shear test. Furthermore this method is applied to the liquefaction analysis of the irregular ground considering the soil-structure interaction.

INTRODUCTION

Recently, many important structures have been constructed on soft irregular grounds. During a major earthquake, the irregular grounds or the surrounding grounds near the structures are considered to shake under cyclic loading with the arbitrary stress path including the principal stress rotation. Therefore, it is important to develop the earthquake response analysis for two-dimensional liquefaction problems. One of the authors proposed the liquefaction analysis method including the soil-structure interaction based on an implicit-explicit finite element method (Ref. 1). In this paper, the formulation of the constitutive equation is presented and the liquefaction analysis is performed to investigate the mechanism of non-linear behavior and liquefaction for soft irregular grounds.

CONSTITUTIVE EQUATION OF SOIL

Soil elements in the ground are subject to repeated loading along the arbitrary stress path including the principal stress rotation caused by irregularity of the ground and existence of structures. The existing constitutive relations based on the theory of plasticity however, are mostly formulated as a function of the stress invariants. Therefore, the relationship between the general stresses (σ_x , σ_y , τ_{xy}) and stress invariants (ϕ_{mo} , τ_{oct} etc.) is not clear, and the stress-strain-dilatancy relationship of soil under an arbitrary stress condition including the principal stress rotation can not be formulated precisely. Hence the constitutive model is proposed as an extension of the Matsuoka's model.

Matsuoka's model Matsuoka proposed the constitutive equation of soil which can evaluate the yielding due to the principal stress rotation (Ref. 2). This Matsuoka's model is derived from the hyperbolic relationship between the general shear-normal stress ratio (τ_{xy}/σ_x or τ_{yx}/σ_y) and the general shear strain (γ_{xy}), and from the "stress-dilatancy relationship" expressed in the general coordinate. The three stress parameters used in this model are shown in Fig. 1 and Eq. (1).

$$\phi_{mo} = \tan^{-1} \frac{\left(\frac{\sigma_x - \sigma_y}{2}\right)^2 + \tau_{xy}^2}{\sigma_x \cdot \sigma_y - \tau_{xy}^2}, \quad \alpha = \frac{1}{2} \tan^{-1} \left(\frac{2\tau_{xy}}{\sigma_x - \sigma_y} \right), \quad \sigma_m = \frac{1}{2} (\sigma_x + \sigma_y) \quad (1)$$

These parameters, ϕ_{mo} , α and σ_m are related to "shearing", "rotation of principal stress axes" and "consolidation", respectively. This constitutive model is able to evaluate yieldings due to "shearing", "principal stress rotation", "isotropic consolidation" and "anisotropic consolidation." Total strain increment can be expressed by a summation form of those components. The stress-strain parameters used for the Matsuoka's model are shown in table 1. ϕ denotes the internal friction angle in terms of the effective stress C_c the compression index, C_s the swell index, e_0 the initial void ratio. λ and μ are the parameters for the strain increment ratio and ks_{1st} for the magnitude of strain.

Stress reversal parameter The relationship between the general stresses (σ_x , σ_y , τ_{xy}) and stress invariants (ϕ_{mo} , τ_{oct} etc) are not clearly related each other in repeated shearing. As shown in Fig. 2, the Mohr's stress circle moves in the same way for the two different effective stress path a-b-c and a-b-d expressed by general stress. Thus the constitutive equation formulated only by stress invariants can not distinguish the reversal shearing from the monotonous shearing where the shearing direction does not change. In order to solve this problem, the parameter for the stress reversal, $\frac{1}{2}(\beta_x + \beta_y)$, shown in Fig. 3 is introduced in the constitutive equation (Ref. 3). The stress reversal parameter is defined only by the general stress. β_x and β_y are the angles at the folded points on the general effective stress paths (σ_x vs. τ_{xy} and σ_y vs. τ_{yx}). It is considered that the smaller the value of $\frac{1}{2}(\beta_x + \beta_y)$ is, the more the soil particles move reverse direction. Thus, we can judge the shearing direction by Eqs. (2) and (3) when the stress ratio reverses. The condition for the reversal shearing is expressed as follows:

$$\text{stress ratio increment} < 0 \quad \text{or} \quad \frac{\beta_x + \beta_y}{2} < 90^\circ \quad (2)$$

Also the condition of monotonous shearing is expressed as follows:

$$\text{stress ratio increment} > 0 \quad \text{and} \quad \frac{\beta_x + \beta_y}{2} \geq 90^\circ \quad (3)$$

Based on the above mentioned rule, we can easily judge the shearing direction in Fig. 2. It is concluded that the relationship between path a-b and path b-c is the reversal shearing and the relationship between path a-b and path b-d is the monotonous shearing.

The Stress reversal parameter is incorporated into the Matsuoka's model and we extended the Matsuoka's model to the arbitrary stress condition. In such a case, ϕ_{mo} is considered as the stress ratio. The proposed stress reversal parameter enables us to apply the constitutive equations formulated by the stress invariants to the arbitrary stress condition. The stress reversal parameter can be introduced to any other constitutive equations as well as the Matsuoka's model. Based on the rule above mentioned, we can calculate the soil behavior regardless of its stress condition.

SIMULATION OF SIMPLE SHEAR TEST

Simulation of a simple shear test is carried out to demonstrate the accuracy of the present constitutive model. The K_0 value of 0.5 and 1.0 are adopted as an example. Note that σ_m , σ_x and σ_y indicate the effective mean stress, effective vertical stress and effective horizontal stress, respectively. Figures 4 and 5 show the comparison between the calculated and the measured results of an undrained simple shear test. A Japanese standard sand called Toyoura sand is used as a test material with relative density $D_r=70\%$. The calculated values are obtained under the condition of no vertical strain increment and no volumetric strain increment. The calculated results for $K_0=0.5$ coincide well with those by the experiment, and the cyclic mobility and hard-spring-type hysteresis loop can be represented. Figure 6 shows the calculated effective stress path in the stress-deviation field $\{\tau_{xy}$ vs. $\frac{1}{2}(\sigma_x - \sigma_y)\}$. It is recognized that the K_0 value changed gradually from 0.5 to 1.0, and the effect of the principal stress rotation is seen especially in the initial stage. Figure 7 demonstrates the calculated results along with the measured ones by the relationship between the stress ratio (τ_{xy}/σ_x or τ_{xy}/σ_m) and the number of cycles to cause liquefaction (DA=4%). It is pointed out from the calculated results that the larger the K_0 value is, the higher the liquefaction potential becomes if the stress ratio τ_{xy}/σ_{x0} is adopted. However, the stress ratio τ_{xy}/σ_{m0} is almost the same irrespective of the K_0 value. This tendency is also pointed out by Ishihara et al. (Ref. 4) from the experiment and Nishi et al. (Ref. 5) from the calculation.

The stress-strain parameters used for these calculations are determined from a conventional triaxial test and an oedometer test (Ref. 2) and those values are shown in table 1. The experimental results are performed by Matsuoka et al (Ref. 3).

LIQUEFACTION ANALYSIS INCLUDING SOIL-STRUCTURE INTERACTION

The present effective stress method based on an implicit-explicit finite element method is proposed in the author's recent paper (Ref. 1). In the hybrid method, the internal force of pore fluid is considered in the equation of motion for granular solid in order to satisfy the undrained condition. The dissipation of excess pore water pressure is not considered. The excess pore water pressure under the undrained condition is obtained from the condition of no volumetric strain increment.

The present method is applied to examine the two-dimensional liquefaction problem including soil-structure interaction. Figure 8 shows a model of an embedded structure used for analysis. The backfill consists of Toyoura sand above mentioned and Matsuoka's model is employed under undrained condition. The stress-strain parameters in the backfill are shown in Table 1 and they are the same as those used in the simple shear simulation. The unit weight of the backfill, basement rock and structure are 1.8tf/m^3 , 2.0tf/m^3 and 1.0tf/m^3 , respectively. The shear wave velocity of the basement rock and structure are 500m/s and 1200m/s , respectively. The absorbing boundary (Ref. 6) is used for the lateral boundary and the Lysmer damper (Ref. 7) is applied to the bottom boundary. El-Centro earthquake with maximum velocity of 20 kine is considered as an incident motion to the bottom boundary through the Lysmer damper.

Figures 9, 10 and 11 show the calculated time histories of acceleration, shear stress and shear strain in the backfill. It is recognized that the amplitudes of the shear stress gradually decrease after 5sec because of liquefaction, on the other hand the shear strain become large especially in element S1. The acceleration of the backfill surface (A2 and A4) becomes large,

but after 6 sec decrease due to liquefaction. It is also found that the acceleration amplitude in the backfill after 5sec does not decrease compared with the shear stress amplitude. This fact can be explained that the longitudinal wave is produced by the shearing of the structure and the wave propagates horizontally in the water. But the shear wave is not transmitted vertically from the base due to liquefaction. Figure 12 shows the hysteresis loop and effective stress paths at element S1. The principal stress rotation and vertical motion are observed at the element S1 in its stress path shown in the stress-deviation field. The effect of the principal stress rotation is about 10 to 20% from the viewpoint of the cumulative shear strain. Figure 13 shows the distribution of the maximum shear strain in the backfill, and it is recognized that the shear strain is large at the surface of the backfill due to liquefaction.

CONCLUSIONS

The stress reversal parameter, $\frac{1}{2}(\beta_x + \beta_y)$, is proposed to distinguish the reversal shearing from the monotonous shearing, and the proposed parameter is incorporated into the Matsuoka's model. First, the accuracy of the present method is discussed through the comparison of simulated and experimental results for the simple shear test under various K_0 conditions. The numerical results are in good agreement with those by the experiments, and the cyclic mobility and hard-spring-type hysteresis loop can be represented. Secondly, the authors performed liquefaction analysis including the embedded rigid structure. It is recognized that the present constitutive model can well represent the response of the irregular ground and the liquefaction. It is also found from the two-dimensional liquefaction analysis that the influence of the principal stress rotation is not neglected.

Consequently, it is concluded that the present method can well simulate the non-linear behavior of the irregular soft ground and soil-structure interaction under arbitrary stress paths. However the results obtained from the analysis are limited. A further investigation based on the earthquake observation and theoretical study may be required.

REFERENCES

1. Ohtsuki, A. and Itoh, T., "Two dimensional effective stress analysis of liquefaction including soil-structure interaction," Earthquake Eng. Struct. Dyn., Vol.15 No.3, 345-366, (1987)
2. Matsuoka, H. and Sakakibara, K., "A constitutive model for sands and clays evaluating principal stress rotation," Soils and Foundations, Vol.27 No.4, 73-88, (1987)
3. Fukutake, K., Ohtsuki, A. and Takewaki, N., "Constitutive Model of Soil under Arbitrary Stress Condition and Its Application to Liquefaction analysis," Seventh Japan Earthquake Engineering Symposium, 691-696, (1986)
4. Ishihara, K. and S, Li., "Liquefaction of saturated sand in triaxial torsion shear test," Soils and Foundations, Vol.12, no.2, 19-39, (1977)
5. Nishi, K., Tohma, J. and Kanatani, M., "Effective stress response analysis for level sand deposits with cyclic mobility," Fifth International Conference on Numerical Methods in Geomechanics, 389-397, (1985)
6. Kunar, R.R. and Rodriguez-Ovejero, L., "A model with non-reflecting boundaries for use in explicit soil-structure interaction analysis," Earthquake Eng.Struct.Dyn., Vol.8, 361-374, (1980)
7. Lysmer, J. and Kuhlemeyer, K.L., "Finite dynamic model for infinite media," J.Eng.Mech.Div., ASCE, Vol.95, NO.EM4, 859-877, (1969)

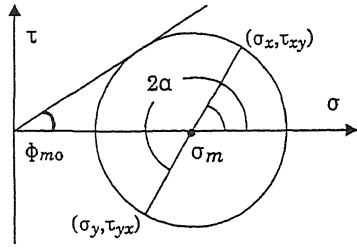


Fig. 1 Three stress parameters, ϕ_{m0} , α and σ_m used in Matsuoka's model

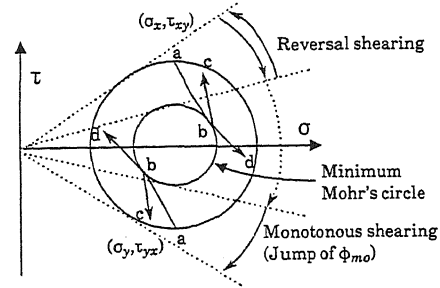


Fig. 2 Judgement of shearing direction

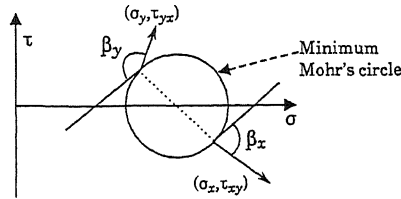


Fig. 3 Schematic diagram of parameter for stress reversal: $\frac{\beta_x + \beta_y}{2}$

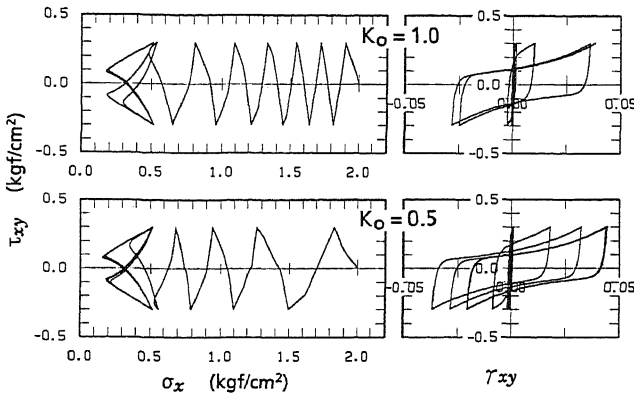
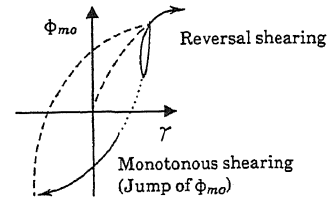


Fig. 4 Calculated effective stress path and stress-strain relation in undrained simple shearing

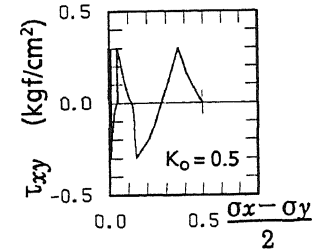


Fig. 6 Calculated effective stress path in stress-deviation field $\{\tau_{xy} \sim \frac{1}{2}(\sigma_x - \sigma_y)\}$

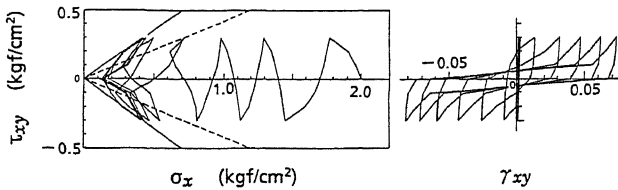


Fig. 5 Measured effective stress path and stress-strain relation in undrained simple shear test (after Matsuoka et al.)

Table 1 Parameters for Toyoura sand ($D_r \approx 70\%$)

ϕ	λ	μ	k_{s1st}	$\frac{Cc}{1+e_0}$	$\frac{Cs}{1+e_0}$
40°	1.2	0.2	0.0023	0.009	0.006

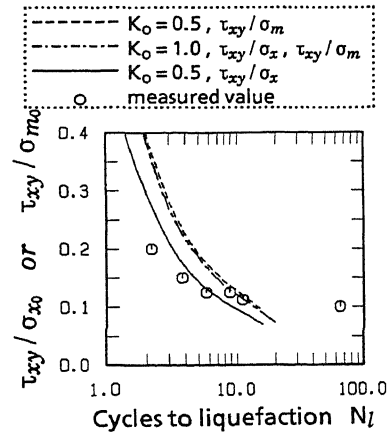


Fig. 7 Stress ratio vs. number of cycles to cause liquefaction (DA = 4%)

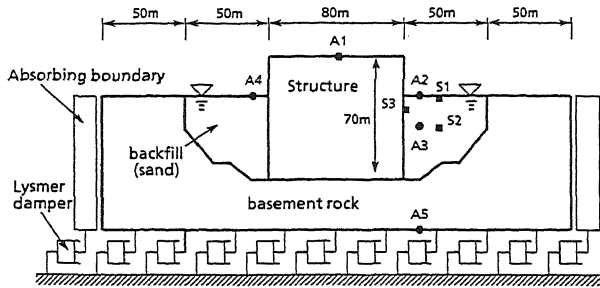


Fig. 8 Model of embedded structure used for liquefaction analysis

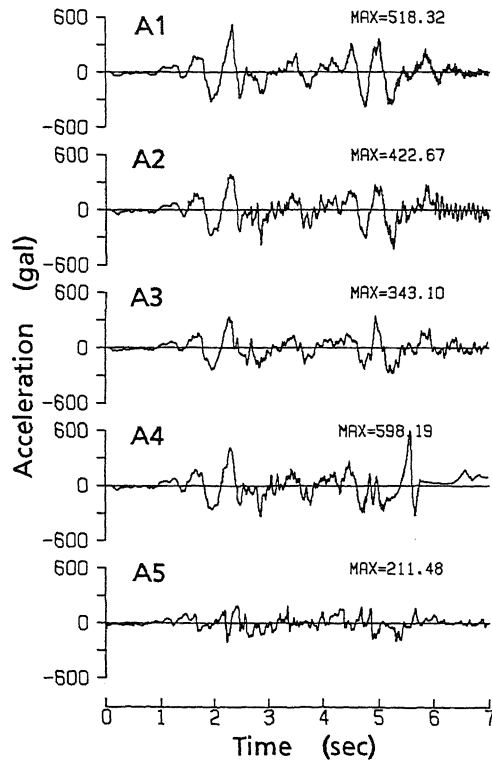


Fig. 9 Time histories of acceleration

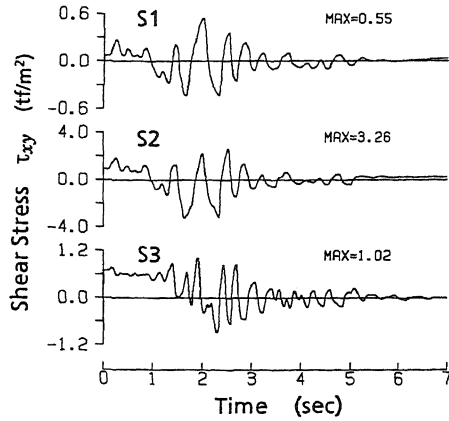


Fig. 10 Time histories of shear stress

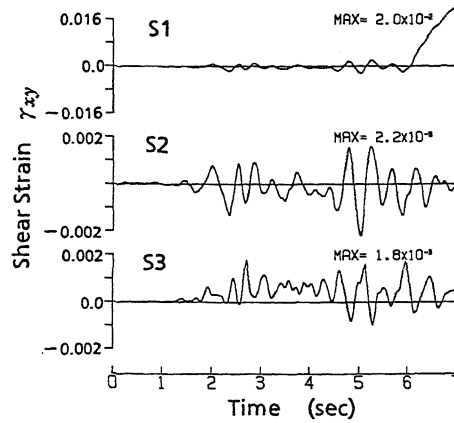


Fig. 11 Time histories of shear strain

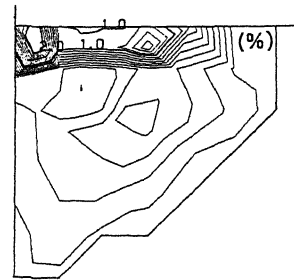


Fig. 13 Distribution of maximum shear strain in backfill

Fig. 12 Effective stress paths and stress-strain relationship at element S1

